

Effect of Sustained Joint Loading on TMJ Disc Nutrient Environment

Y. Wu, S.E. Cisewski, M.C. Coombs, M.H. Brown, F. Wei, X. She, M.J. Kern, Y.M. Gonzalez, L.M. Gallo, V. Colombo, L.R. Iwasaki, J.C. Nickel, and H. Yao

APPENDIX

This appendix describes the detailed derivation of the diffusion governing equations and constitutive relationships for the finite element (FE) modeling.

Theoretical Formulation

Fick's diffusion equation was used to model solute transport and nutrient metabolism in the TMJ disc (Selard et al. 2003; Wu et al. 2013):

$$\frac{\partial c^s}{\partial t} + D^s \left[\frac{\partial^2 c^s}{\partial x^2} + \frac{\partial^2 c^s}{\partial y^2} + \frac{\partial^2 c^s}{\partial z^2} \right] = Q^s \quad (1)$$

Where c^s is the solute concentration (s: glucose, lactate, and oxygen), D^s is the diffusivity of each nutrient solute measured from the *in vitro* diffusion experiments, and Q^s is the energy metabolic rate defined by the Michaelis-Menten kinetics equation (Guehring et al. 2009; Huang et al. 2007; Kuo et al. 2011a; Zhou et al. 2004).

$$Q^{glucose} = -\rho^{cell} \frac{V_{max}^{glucose} \times c^{glucose}}{k_m^{glucose} + c^{glucose}} \quad (2)$$

$$Q^{oxygen} = -\rho^{cell} \frac{V_{max}^{oxygen} \times c^{oxygen}}{k_m^{oxygen} + c^{oxygen}} \quad (3)$$

Where V_{max} is the maximum cellular nutrient metabolic rate, k_m is the nutrient solute concentration at which the cellular nutrient metabolic rate drops to 50% of V_{max} , and ρ^{cell} is the TMJ disc cell density. Negative metabolic rates indicate nutrient consumption.

The lactate production rate (LPR) was predicted using glucose and oxygen consumption rates according to the stoichiometry of intracellular energy metabolic reactions (Venkatasubramanian et al. 2006), where the uptake of one glucose molecule produces two lactate molecules, and the oxidation of one lactate molecule requires three oxygen molecules.

$$Q^{lactate} = -2Q^{glucose} + \frac{1}{3}Q^{oxygen} \quad (4)$$

A linear relationship between pH and lactate concentration was used to calculate pH values within the TMJ disc (Bibby et al. 2005; Selard et al. 2003).

$$pH = -0.1c^{lactate} + 7.5 \quad (5)$$

Furthermore, viable cell density, which depends on nutrient availability, was predicted using a theoretical framework from fibrocartilage cells (Zhu et al. 2012).

$$\frac{\partial \rho^{cell}}{\partial t} = \alpha \left(\frac{c^{glucose} - c_{critical}^{glucose}}{c^{glucose} + k_1} - \frac{|c^{glucose} - c_{critical}^{glucose}|}{c^{glucose} + k_2} \right) \times \rho^{cell} \quad (6)$$

Where $c_{critical}^{glucose}$ is the threshold glucose level necessary for TMJ disc cell survival. The rate of normalized cell density change depends on parameters α , k_1 , and k_2 which can be determined from the biology of cartilaginous cells.

Tissue and Cell Properties

The Michaelis-Menten (M-M) kinetics parameters (V_{max} , K_m) for glucose consumption were collected by curve fitting glucose metabolic rates under varying glucose concentrations in this study (Appendix Fig. 1). V_{max} was defined as 18 nmol/million cells/hr under all oxygen levels, while a piecewise function was used for K_m under varying oxygen conditions [0-2.5% oxygen: $K_m=0.8$ mM; 2.5-5% oxygen: $K_m=1.6$ mM (average between low and high); 5-6% oxygen: $K_m=2.3$ mM] (Appendix Table 1). The M-M parameters for oxygen consumption in the

TMJ disc were collected from our previous study ($V_{\max}=28.7$ nmol/million cells/hr; $K_m=0.019$ mM) (Kuo et al. 2011a). The lactate production rates were determined from the consumption rates of glucose and oxygen according to stoichiometry of intracellular energy metabolic reactions (Equation 4). Additionally, experimentally determined lactate production rates from the study *in vitro* cellular metabolic measurements were used to validate the theoretical lactate production rates determined by stoichiometry of intracellular energy metabolic reactions. Using Equation 2-4, theoretical lactate production rates under *in vitro* tissue explant culture conditions were calculated and found to be consistent with experimental measurements (Appendix Fig. 2).

FE model strain dependent glucose and lactate diffusivities under 0% and 20% strain were collected from the *in vitro* solute diffusion experiments in this study (0% strain: $D^{\text{glucose}}=4.7 \times 10^{-7}$ cm²/sec; $D^{\text{lactate}}=7.9 \times 10^{-7}$ cm²/sec; 20% strain: $D^{\text{glucose}}=2.7 \times 10^{-7}$ cm²/sec; $D^{\text{lactate}}=5.2 \times 10^{-7}$ cm²/sec). For small solute diffusivity in fibrocartilage tissues, an empirical constitutive relation was followed: $D_{\text{tissue}}/D_{\text{aqu}}=A\Phi^2$ (Urban et al. 1977), where Φ is the tissue volume fraction of water. According to the strain dependent diffusivities of glucose and lactate for the TMJ disc measured in this study, A is 0.11, with Φ equal to 0.70 for TMJ disc tissue (Kuo et al. 2011b; Wright et al. 2013). Therefore, oxygen diffusivities in the TMJ disc under different strain levels were calculated using the reported diffusivity value in water ($D_{\text{aqu}}^{\text{oxygen}}=3 \times 10^{-5}$ cm²/s) (Huang and Gu 2008) as the base for estimation (0% strain: $D^{\text{oxygen}}=16.2 \times 10^{-7}$ cm²/sec; 20% strain: $D^{\text{oxygen}}=11.2 \times 10^{-7}$ cm²/sec).

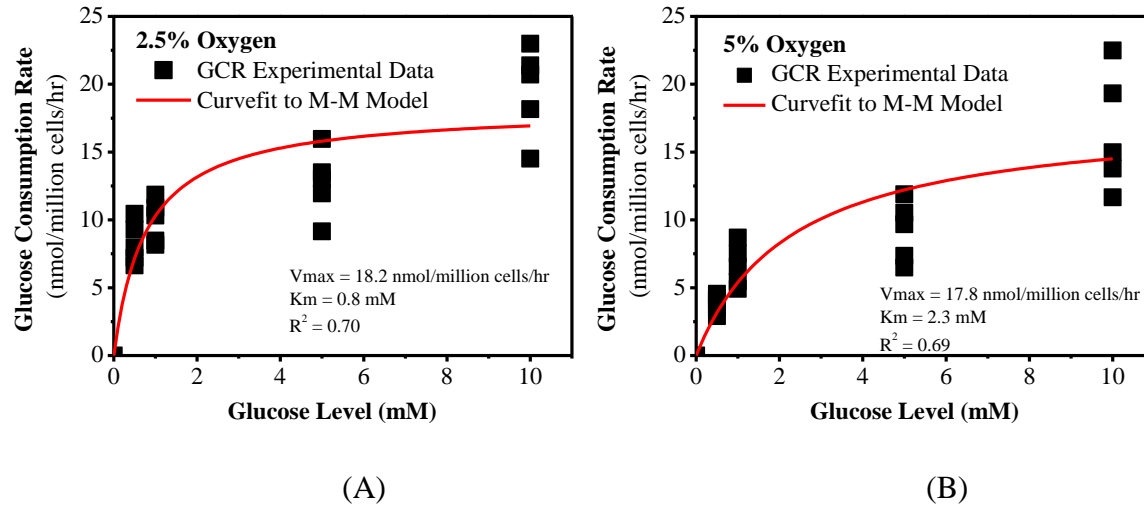
According to previous experimental studies, fibrocartilaginous cells start to die when glucose levels fall below 0.5 mM, and below 0.2 mM all cells die within three days (Bibby et al. 2002; Bibby and Urban 2004; Horner and Urban 2001), therefore $c_{\text{critical}}^{\text{glucose}}=0.5$ mM, $k_1=k_2=0.2$,

and $\alpha=1/\text{day}$ (Zhu et al. 2012). Initial cell density in the healthy TMJ disc was reported in our previous study ($\rho_0^{\text{cell}}=50$ million cells/mL) (Kuo et al. 2011a) (Appendix Table 1).

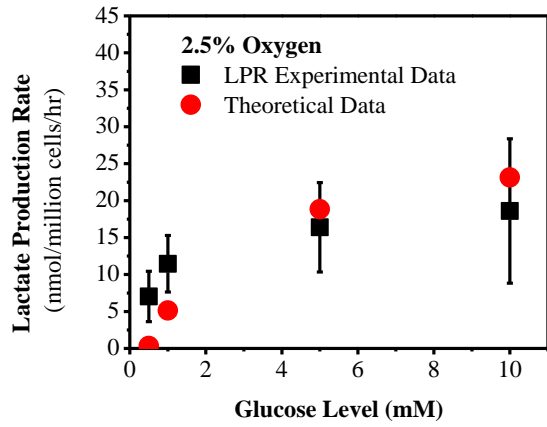
Boundary and Initial Conditions

For healthy unloaded TMJ discs, the glucose, lactate, and oxygen concentrations on the disc boundary in FE models were 4 mM, 0.9 mM, and 6%, respectively (Selard et al. 2003; Wu et al. 2013). For healthy loaded TMJ discs, impermeable boundary conditions (molar flux of nutrient solutes $n \cdot J^s = 0$; s: glucose, lactate, and oxygen) were used for the superior and inferior loading areas to mimic localized blocking of solute exchange under sustained joint loading conditions (Appendix Table 1).

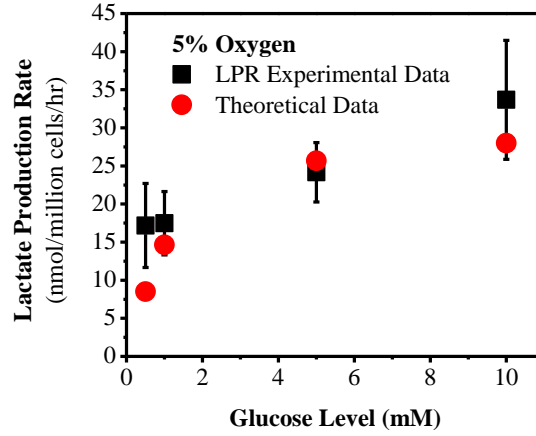
For each human TMJ disc, the nutrient profiles under the unloaded condition were simulated using the stationary solver in commercial FE software (COMSOL, Burlington, MA). By switching the boundary conditions in the loading areas to impermeable and using strain dependent solute diffusivities, the nutrient profiles in the loaded discs were simulated using the time-dependent solver in this software. A 4-hour loading period was simulated to investigate the effect of sustained joint loading on TMJ disc nutrient environment. The equilibrium nutrient profiles in the unloaded disc were used as the initial conditions for the simulations in the loaded disc.



Appendix Figure 1. Glucose consumption rates (GCR) of TMJ disc cells curve fit to the M-M model for V_{max} and K_m at 2.5% (A) and 5% (B) oxygen levels. Sample size $n=40$ porcine TMJ discs ($n=5$ discs for GCR experimental runs under each nutrient condition).



(A)



(B)

Appendix Figure 2. Comparison of lactate production rates (LPR) of TMJ disc cells between experimental data and theoretical predictions at 2.5% (A) and 5% (B) oxygen levels. Sample size n=40 porcine TMJ discs (n=5 discs for LPR experimental runs under each nutrient condition).

Appendix Table 1. Simulation parameters used in the FE model of TMJ disc.

Material Properties	Glucose	Oxygen	Lactate
Metabolic Rate: V_{\max} (nmol/million cells/hr)	18 (0-6% oxygen)	28.7 ^a	Predicted from consumption rates of glucose and oxygen using Equation 4 ^b
Metabolic Rate: K_m (mM)	0.8 (0-2.5% oxygen)	0.019 ^a	
	1.6 (2.5-5% oxygen)		
Diffusivity: D^s (10^{-7} cm ² /sec)	2.3 (5-6% oxygen)	16.2 (0% strain)	7.9 (0% strain)
	4.7 (0% strain)	11.2 (20% strain)	5.2 (20% strain)
Boundary Conditions			
Unloaded Area (mM)	4 ^{c,d}	0.06 ^{c,d}	0.9 ^{c,d}
Loaded Area (mM)	Impermeable ($\mathbf{n} \cdot \mathbf{J}^{\text{glucose}} = \mathbf{n} \cdot \mathbf{J}^{\text{lactate}} = \mathbf{n} \cdot \mathbf{J}^{\text{oxygen}} = 0$) ^{e,f,g}		
Initial Conditions			
Unloaded Disc (mM)	4 ^{c,d}	0.06 ^{c,d}	0.9 ^{c,d}
Loaded Disc (mM)	The equilibrium nutrient profiles in the unloaded disc		

^a (Kuo et al. 2011a)

^b (Venkatasubramanian et al. 2006)

^{c,d} (Selard et al. 2003; Wu et al. 2013)

^{e,f,g} (Huang and Gu 2008; Yao and Gu 2004; Zhu et al. 2012)

References

- Bibby SR, Fairbank JC, Urban MR, Urban JP. 2002. Cell viability in scoliotic discs in relation to disc deformity and nutrient levels. *Spine*. 27(20):2220-2228.
- Bibby SR, Jones DA, Ripley RM, Urban JP. 2005. Metabolism of the intervertebral disc: Effects of low levels of oxygen, glucose, and ph on rates of energy metabolism of bovine nucleus pulposus cells. *Spine*. 30(5):487-496.
- Bibby SR, Urban JP. 2004. Effect of nutrient deprivation on the viability of intervertebral disc cells. *Eur Spine J*. 13(8):695-701.
- Guehring T, Wilde G, Sumner M, Grunhagen T, Karney GB, Tirlapur UK, Urban JP. 2009. Notochordal intervertebral disc cells: Sensitivity to nutrient deprivation. *Arthritis Rheum*. 60(4):1026-1034.
- Horner HA, Urban JP. 2001. 2001 volvo award winner in basic science studies: Effect of nutrient supply on the viability of cells from the nucleus pulposus of the intervertebral disc. *Spine*. 26(23):2543-2549.
- Huang CY, Gu WY. 2008. Effects of mechanical compression on metabolism and distribution of oxygen and lactate in intervertebral disc. *J Biomech*. 41(6):1184-1196.
- Huang CY, Yuan TY, Jackson AR, Hazbun L, Fraker C, Gu WY. 2007. Effects of low glucose concentrations on oxygen consumption rates of intervertebral disc cells. *Spine*. 32(19):2063-2069.
- Kuo J, Shi C, Cisewski S, Zhang L, Kern MJ, Yao H. 2011a. Regional cell density distribution and oxygen consumption rates in porcine tmj discs: An explant study. *Osteoarthritis Cartilage*. 19(7):911-918.
- Kuo J, Wright GJ, Bach DE, Slate EH, Yao H. 2011b. Effect of mechanical loading on electrical conductivity in porcine tmj discs. *J Dent Res*. 90(10):1216-1220.
- Selard E, Shirazi-Adl A, Urban JP. 2003. Finite element study of nutrient diffusion in the human intervertebral disc. *Spine*. 28(17):1945-1953.
- Urban JP, Holm S, Maroudas A, Nachemson A. 1977. Nutrition of the intervertebral disk. An in vivo study of solute transport. *Clin Orthop Relat Res*. (129):101-114.
- Venkatasubramanian R, Henson MA, Forbes NS. 2006. Incorporating energy metabolism into a growth model of multicellular tumor spheroids. *J Theor Biol*. 242(2):440-453.
- Wright GJ, Kuo J, Shi C, Bacro TR, Slate EH, Yao H. 2013. Effect of mechanical strain on solute diffusion in human tmj discs: An electrical conductivity study. *Ann Biomed Eng*. 41(11):2349-2357.

Wu Y, Cisewski S, Sachs BL, Yao H. 2013. Effect of cartilage endplate on cell based disc regeneration: A finite element analysis. *Mol Cell Biomech.* 10(2):159-182.

Yao H, Gu WY. 2004. Physical signals and solute transport in cartilage under dynamic unconfined compression: Finite element analysis. *Ann Biomed Eng.* 32(3):380-390.

Zhou S, Cui Z, Urban JP. 2004. Factors influencing the oxygen concentration gradient from the synovial surface of articular cartilage to the cartilage-bone interface: A modeling study. *Arthritis Rheum.* 50(12):3915-3924.

Zhu Q, Jackson AR, Gu WY. 2012. Cell viability in intervertebral disc under various nutritional and dynamic loading conditions: 3d finite element analysis. *J Biomech.* 45(16):2769-2777.